Delamination: Thermoplastic (DM 4030SR)

(Perichaud/Fremont)

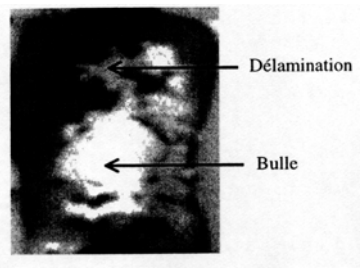

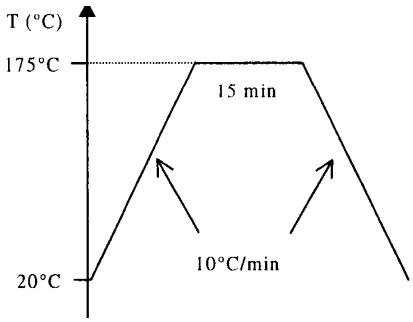

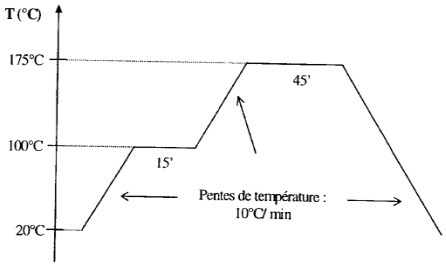

1

3.5 Variable frequency microwave heating curves for different ECAs

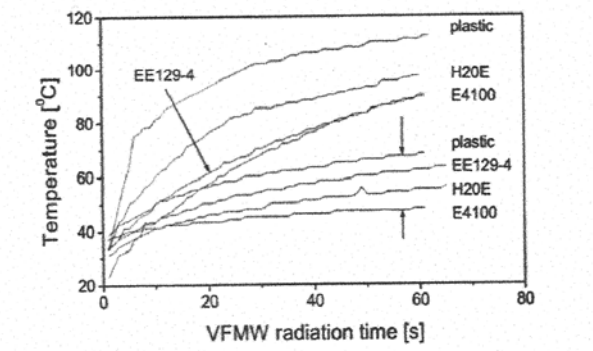

FIG. 5. Heating curves for different ECAs radiated by VFMW at power of 100W(between two vertical arrows) and 300W

4/27/2009

2

ECA Resistance

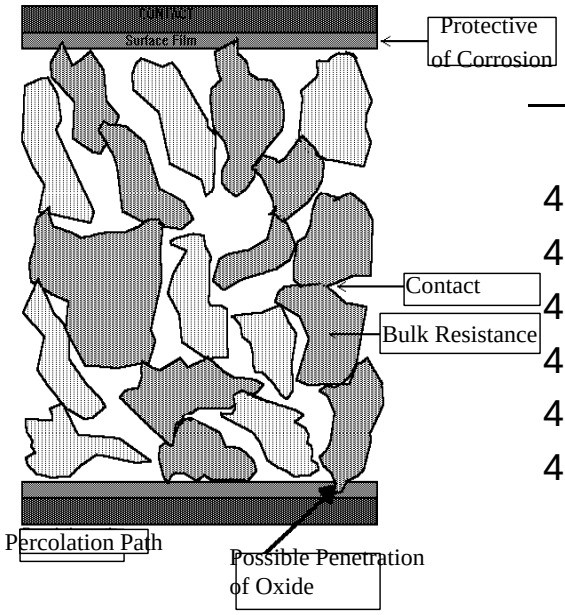

4. ICA Resistance

4.1 Percolation
4.2 Particle
4.3 Inter-particle
4.4 Pad contact
4.5 Experimental
4.6 Modeling

4.1 Monte Carlo Percolation Models

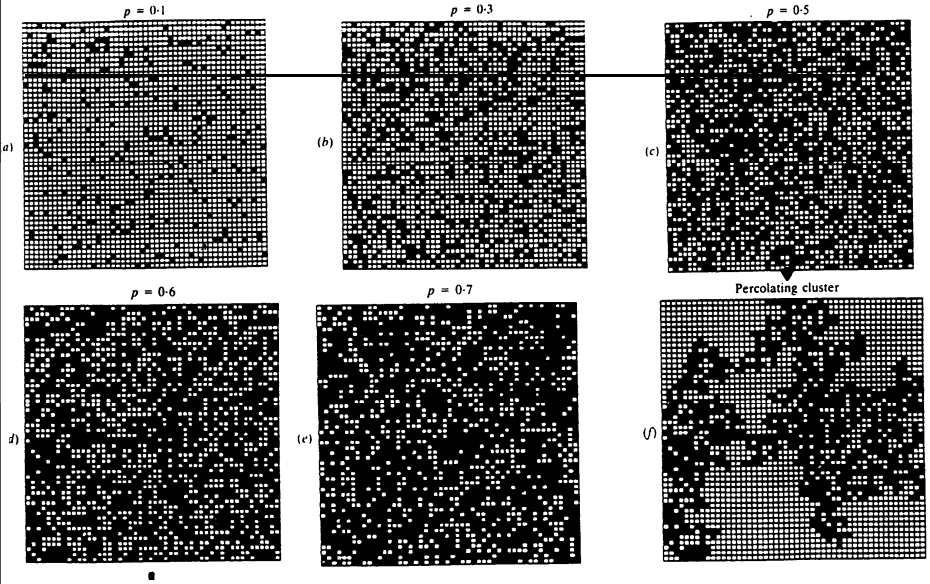

- (Smilauer)

Size effect in percolation

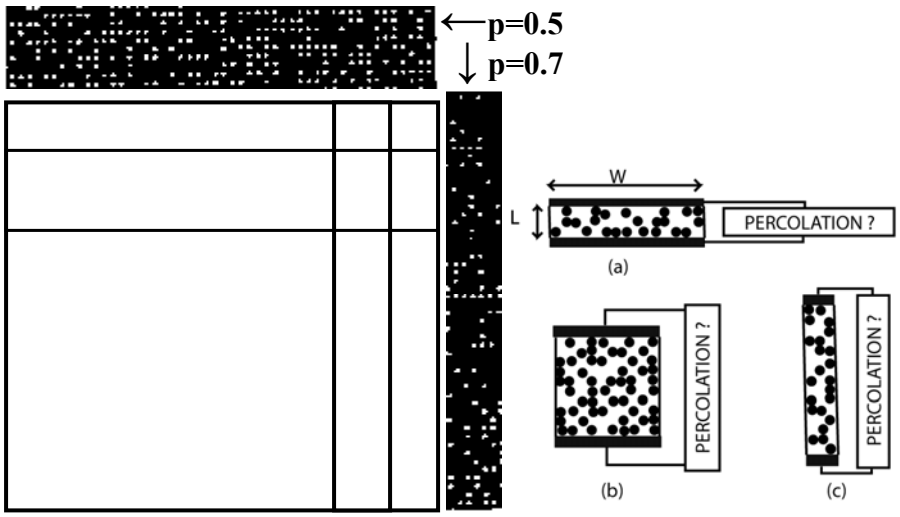

Percolation: Size Effect Dispersion

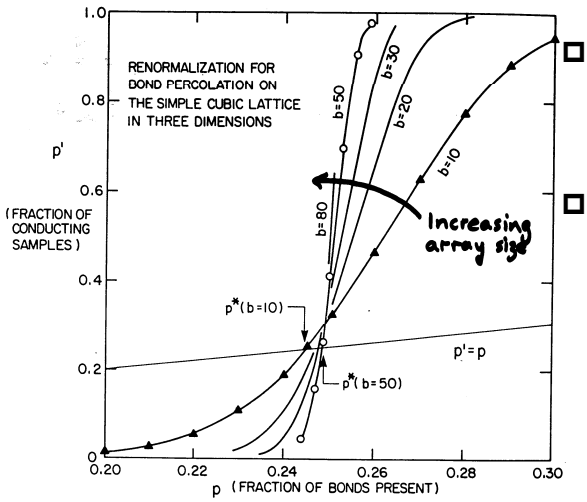

- Averaged simulations
- Reproducibility
  - small sizes
  - incr tolerances
  - higher Ag

4.2 Particle Bulk Resistance

- **Mean free path λ:** $\sigma \propto \lambda$
  - & λ^{-1} = λ^{-1} (lattice (phonon)) + λ^{-1} (impurity, defect, etc grain boundaries) + λ^{-1} (size effects)
  - $\rho \sim \rho_{bulk}$ & $TCR \sim TCR_{bulk}$ if sec scatter neglig.
  - Also $TCR_{size/impurity} \sim 0$
- **Typically λ_{latt} ~ 10's nm (<100nm)**
  - Ag flakes ~ 10's μm diameter, μm thickness
  - Therefore ignore size effects

4.3 Particle Contact Resistance

4.3.1 Constriction resistance: $R = \rho / 2a$

- Current crowding
- Circular contact
- Diameter 2a

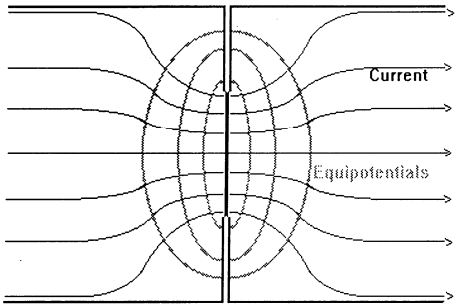

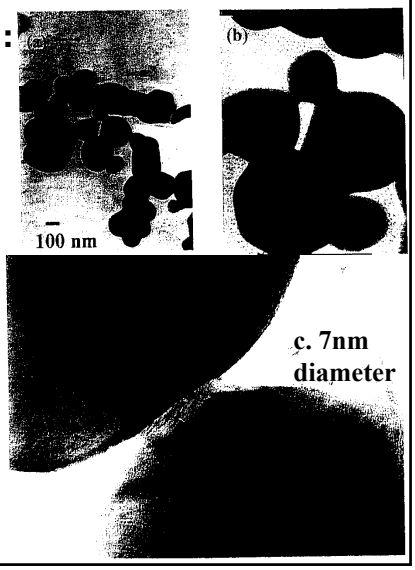

4.3.4 AgO/Ag_2O Degenerate Semiconductor

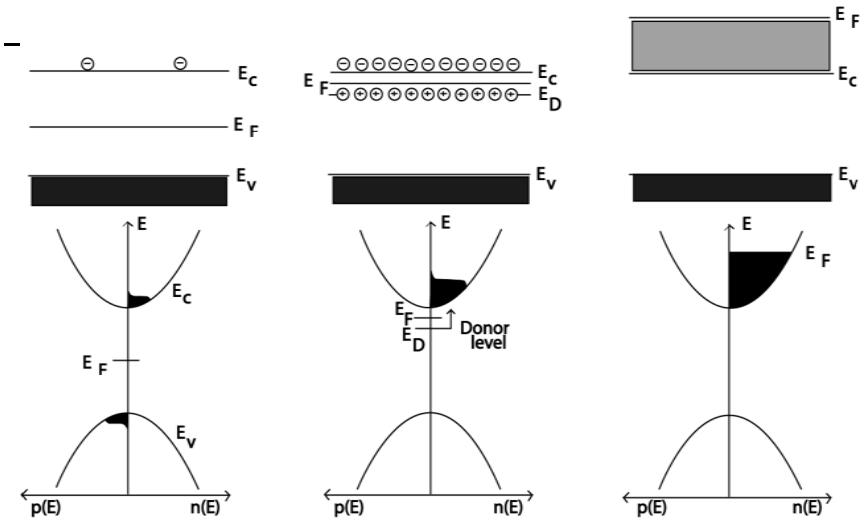

Silver oxide (degenerate semiconductor) Also $\propto 1/a^2$

4.4 Pad contact

- Possible oxide layer
- Penetration by "chestnut" particles
- Dissimilar metals
  - Diffusion
  - Corrosion

4.5. Electrical Properties: Experimental

4.5.1 Temperature coefficient of resistance (TCR)
4.5.2 Frequency effects
4.5.3 Lubricants
4.5.4 Size effect
4.5.5 Noise
4.5.6 Thermoelectric effect

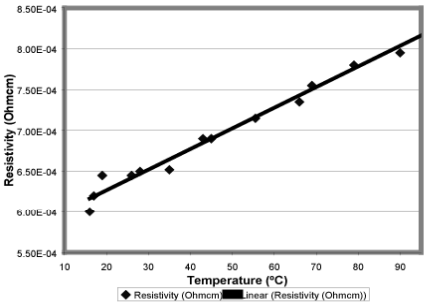

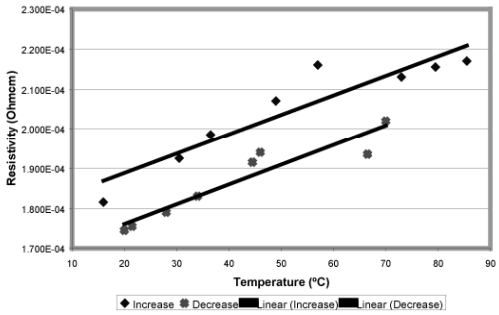

4.5.1 TCR Results

- $TCR_{ICA} \approx TCR_{Ag}$
- $\therefore R_{ICA} \approx R_{Ag}$
- Contact R negligible

Resistivities for various temperatures.

(a) Brass stenciled CT-5047-02 thermoset sample (TCR-0.0039/ºC).

(b) (b) CSM-933-65-1 screen printed thermoplastic sample {TCR=0.0038/ºC}

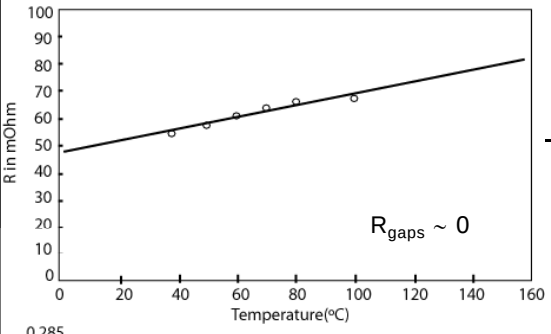

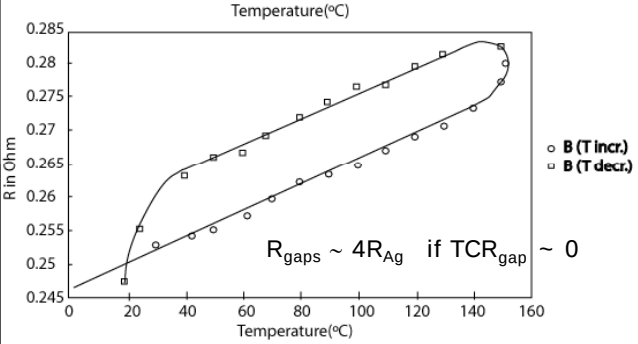

TCR Results

Simple resistivity model

Typical ICA: 20vol% Ag
Divide equally into chains running x, y, z

i.e. $\frac{1}{5}$th vol → $\frac{1}{15}$th in each direction

Hence ideal $15\rho_{Ag}$ minimum value

Typically observe $\rho_{ICA} \approx 15$ to $300\rho_{Ag}$

Ideal → add in dispersion, meandering path

($\rho_{Ag} \approx 1.6\mu\Omega \cdot cm$)

4.5.2 Frequency Effects: Tunnel Gaps

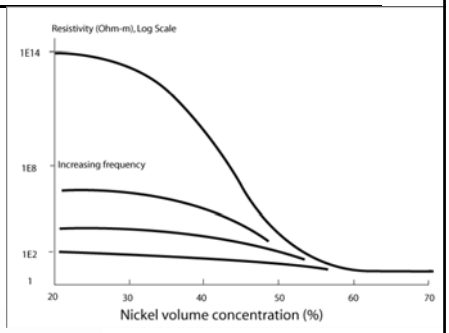

AC Effects: Sub-Threshold

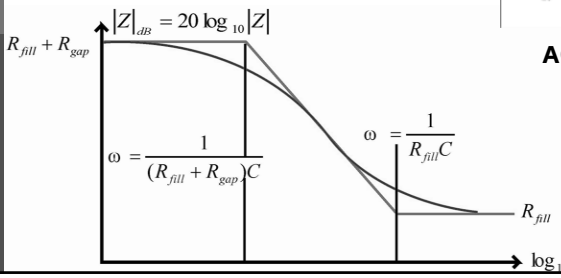

Frequency Effects: Skin Effect

- R

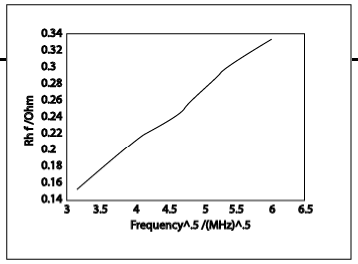

$\sqrt{f}$

This graph shows the linear relationship between the resistance at high frequencies and the square root of frequency

- L

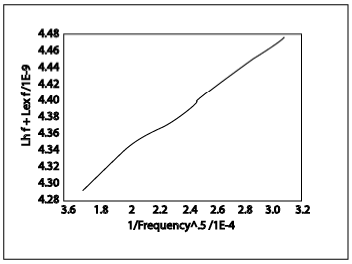

$1/\sqrt{f}$

This figure exhibits the linear relationship of the inductance at high frequencies with f^.5

Skin Effect: Calculation

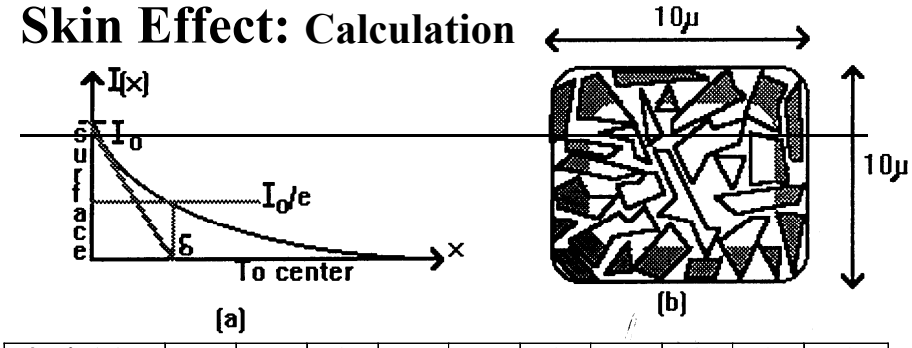

$\log_{10}$ freq(Hz)		1	2	3	4	5	6	7	8	9	10
Ag	δ	0.2cm	6.4mm	2mm	640μm	200μm	64μm	20μm	6.4μm	2μm	0.64μm
	R_{Skin}	0.8μΩ	2.5μΩ	8μΩ	25μΩ	80μΩ	0.25μΩ	0.8mΩ	2.5mΩ	8mΩ	25mΩ
	L_{int}	12.7nH	4nH	1.27nH	0.4nH	127pH	40pH	12.7pH	4pH	1.27pH	0.4pH
Solder	δ	6.4cm	2cm	6.4mm	2mm	640μm	200μm	64μm	20μm	6.4μm	2μm
	R_{Skin}	2.5μΩ	8μΩ	25μΩ	80μΩ	0.25mΩ	0.8mΩ	2.5mΩ	8mΩ	25mΩ	80mΩ
	L_{int}	40nH	12.7nH	4nH	1.27nH	0.4nH	127nH	40pH	12.7pH	4pH	1.27pH

$\rho_{Ag}=1.6\cdot10^{-8}\,\Omega\cdot m$ $\rho_{Solder}=16\cdot10^{-8}\,\Omega\cdot m$

Low frequency: Solder resistance < ICA resistance
High frequency: Solder resistance > ICA resistance
(because areas become the same and $\varrho_{Ag} << \varrho_{solder}$

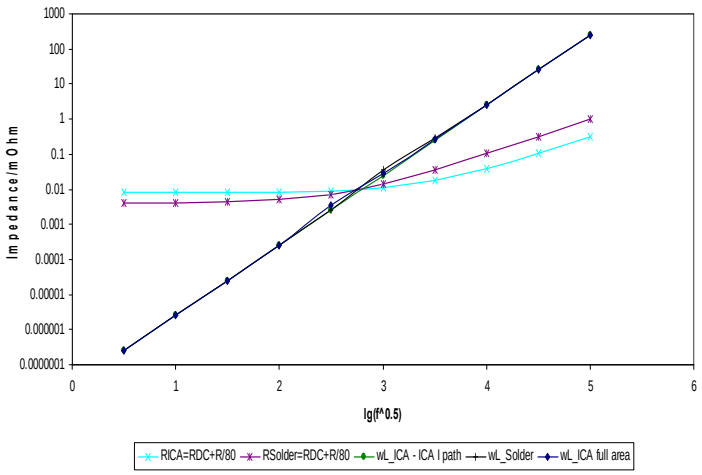

4.5.3 Particle Lubricants & Contacts

- Lubricants added to Ag flakes
- Effect on resistance?
- Apply pressure to Ag flakes
- Conducts with lubricant on surface
- Apply pressure to uncured ICA
- No conduction; resin incompressible
- Resistance drop associated with shrinkage

Carbon on flake surface appears after cure: Changes in peak intensities with temperature during cure

Miragliotta, Benson, Phillips, & Emerson: MRS '01, 2002 Materials

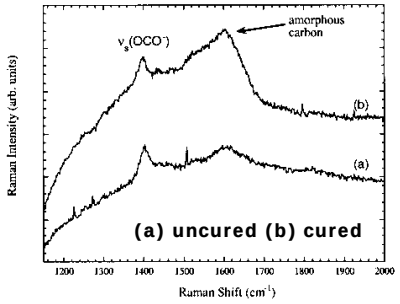

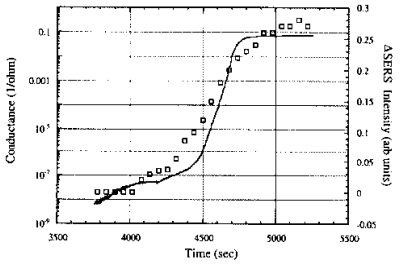

LHS: 1600cm-1 C peak

Figure 6. Change in the peak intensity of the carbon mode at 1600 cm^{-1} in the Raman spectrum from the Ag-filled epoxy. The corresponding sample

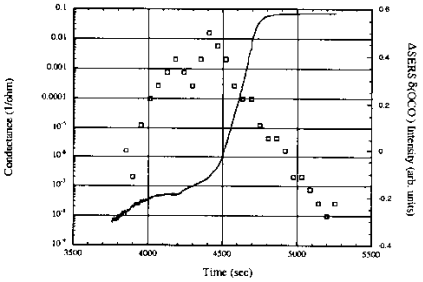

RHS: 744 cm-1 carboxylate peak

Figure 6. Change in the peak intensity of the carboxylate bending mode at 744 cm^{-1} in the Raman spectrum from the Ag-filled epoxy. The

Stearic acid can be removed/replaced by short-chain dicarboxylic acids, with strong affinity for Ag surface (e.g. malonic acid) Li/Moon/Li/Wong ECTC 2004]

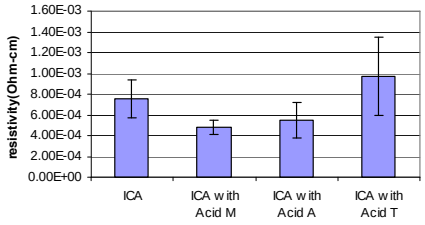

Figure. 5 Effects of different dicarboxylic acids on the conductivity of ICA

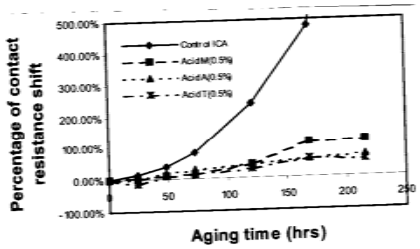

Figure. 6 Contact Resistance Shifts of ECAs with and without dicarboxylic acids

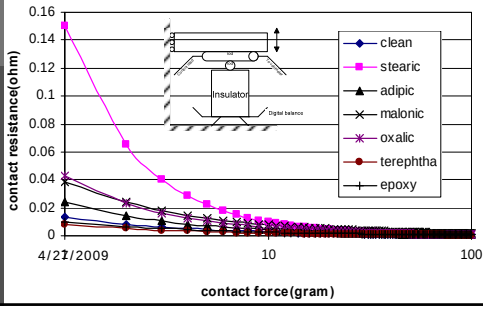

Experimental resistances with short-chain acids

[Qu – APM'05]

Z-axis Size Effect Expt

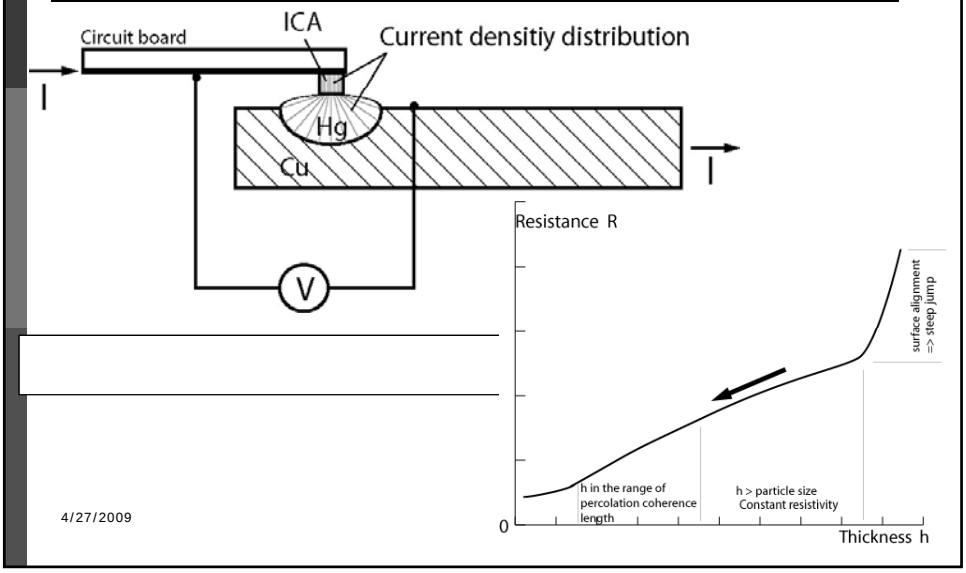

4/27/2009

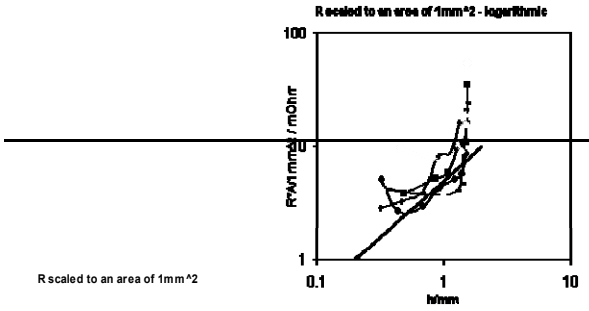

Resistance shown in logarithmic scale including the line of slope for constant resistivity bulk effect

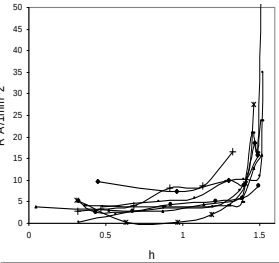

Resistance as a function of the thickness for all samples scaled to a cross section area of 1mm^2.

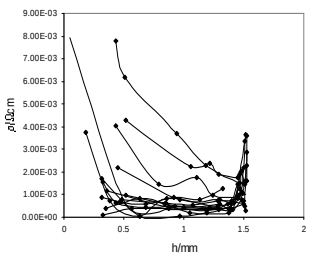

Resistivity as a function of the thickness.

4/27/2009

22

4.5.7 ICA Resistance: Summary

1. Percolation theory and size effects
2. Bulk particle resistance
   - Electron mean free path << particle sizes
3. Particle contact resistance
   - Temperature coefficient of resistance (TCR)
   - $R = R_X + R_{Ag}(T)$
   - Frequency effects
   - Skin effect
   - Lubricant
4. Pad contact effects
   - Corrosion
     - Pad metallurgy: noble metal finishes
   - Galvanic corrosion: Ag to ?? (Sn? Pd? Au?)

4.6. ICA Electrical Conduction Modeling

- 4.6.1 Monte Carlo placement problem
- 4.6.2 Spherical particles (Sancaktar)
  - Position adjust along line of centers
- 4.6.3 Rectangular; xyz orientations (Li/Morris)
  - Seek vacant spot
- 4.6.4 Rectangular; 1° rotations (McCluskey et al)
  - V=1/R potential fields; next ptle at lowest potl
- 4.6.5 Ellipsoids (Nakagawa/Iwamoto/Mustoe)
  - compression algorithm, discrete element
- 4.6.6 Ellipsoids (Mundlein/Nicolics & Qu)
  - compression algorithm, networks

5. Mechanical Properties

- **5.1 Modulus / yield**
  - **Initial wear**
  - **Mechanical cycling**
  - **Dynamic properties**
- **5.2 Adhesion**
  - **Plasma cleaning**
  - **Vacuum treatment**
- **5.3 Impact strength / drop test**
  - **NCMS: 6 drops from 5 ft**
- **5.4 Thermal shock**

Determination of dynamic mechanical properties of Ag ICA

(Wu et al)

Uniaxial nonlinear stress-strain curves for a silver-filled epoxy system

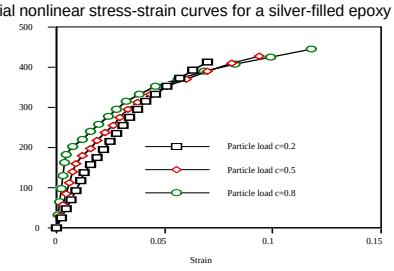

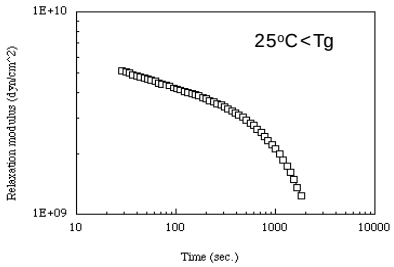

Dynamic shear modulus vs temperature for fully cured ICA

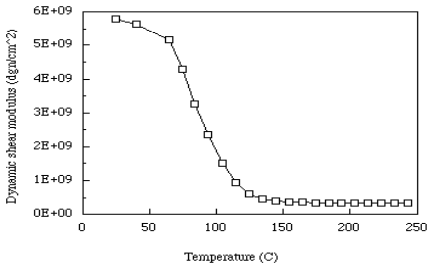

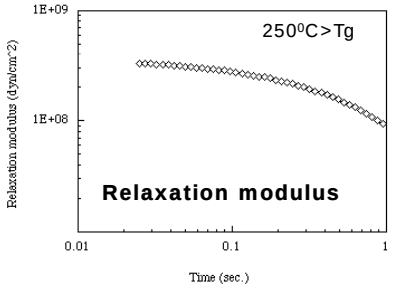

Adhesion

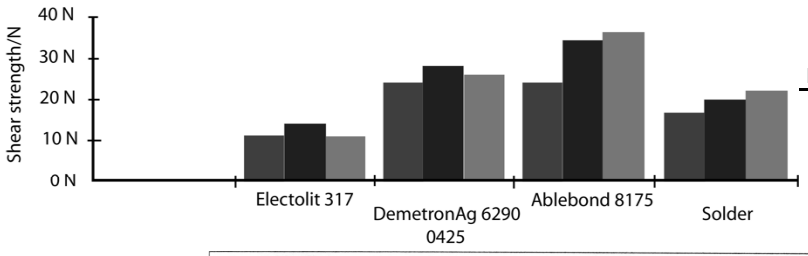

Danfoss

5.2 Adhesion

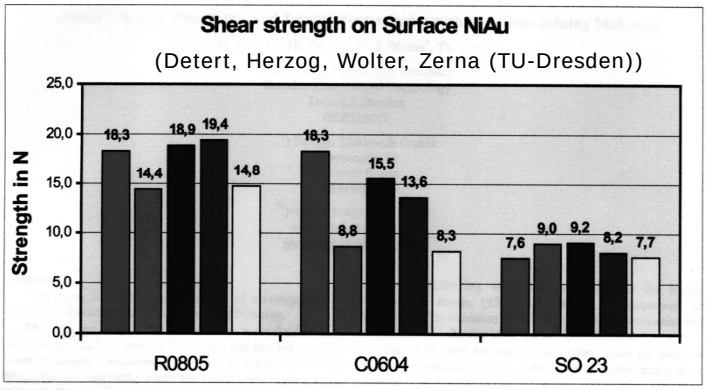

Figure 5: Shear test results for best printing ICA A

4/27/2009

Plasma Cleaning

Wolter et al

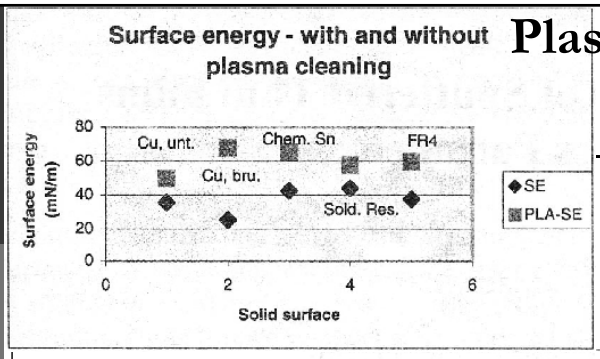

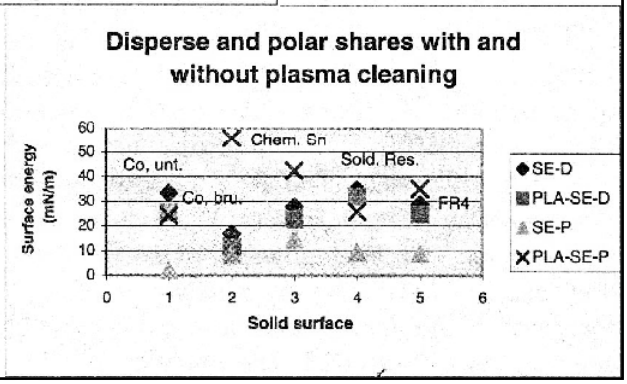

4/27/2009

Shear test result with plasma treatment

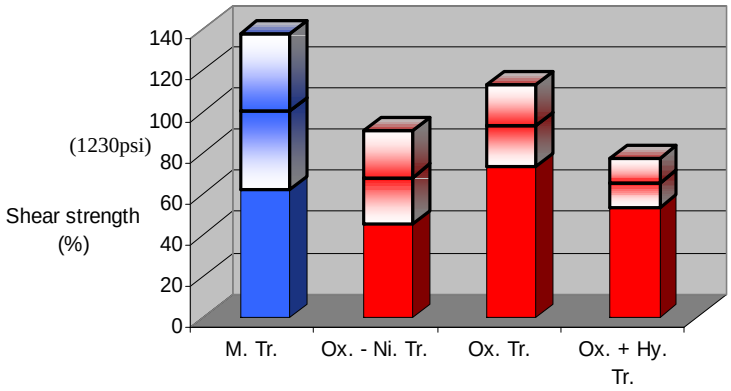

Adhesive before and after vacuum process

ICA before vacuum process

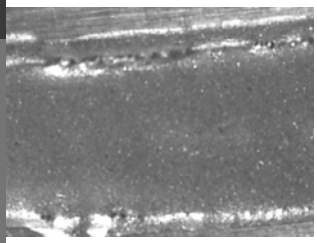

ICA after vacuum process

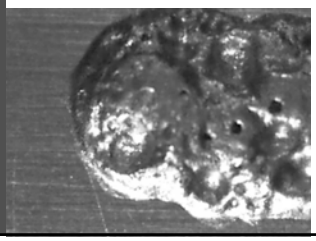

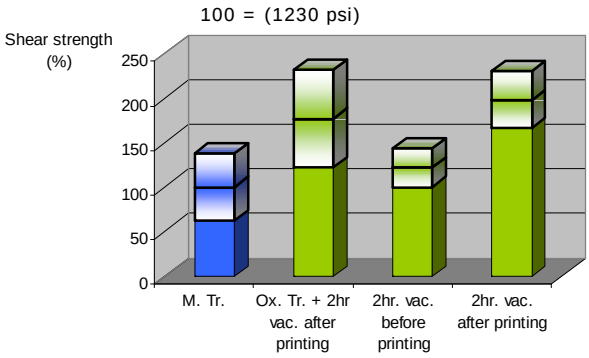

Change of surface by:
- **removal of air and water**
- **contraction of adhesive**

	No Vacuum	Vacuum
Average Resistivity	$4.22 \cdot 10^{-3}\,\Omega\text{cm}$	$2.92 \cdot 10^{-3}\,\Omega\text{cm}$
Standard Deviation	$3.29 \cdot 10^{-3}\,\Omega\text{cm}$	$1.53 \cdot 10^{-3}\,\Omega\text{cm}$

	No Vacuum	Vacuum
Average Pull Test strength	160 N	235 N
Standard Deviation	108 N	56 N

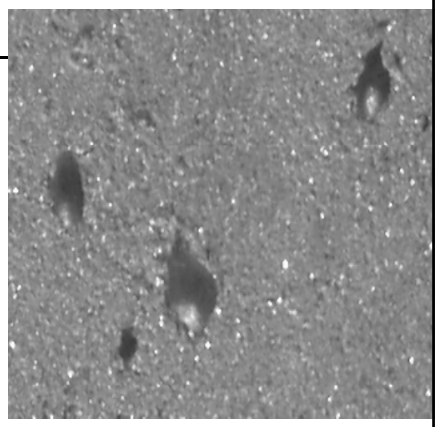

Bubbles on the ICA-Copper-Interface of a vacuum treated sample

4/27/2009 31

Adhesion: Surface Roughness

(Chow, Li, Yuen: 2002 Adv Pkg Materials Sympos

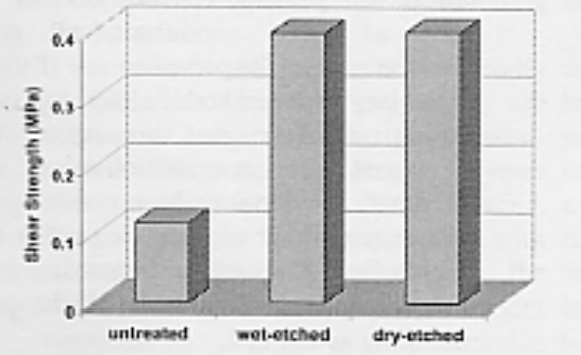

Fig. 3 Die shear test results show adhesion enhancement of PANI on etched Au substrate compared to untreated.

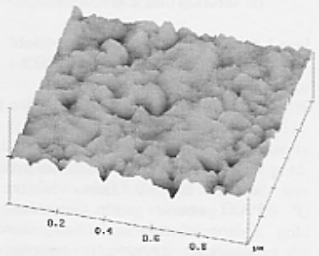

Fig. 4 Typical surface topographic image of untreated gold substrates

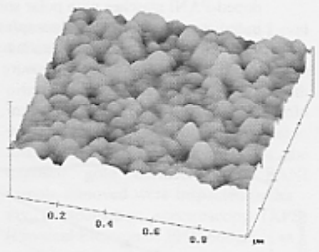

Fig. 5 Typical surface topographic image of etched gold substrates.

E-Pads & Add Carbon Fibers

(Keil, Bjarnason, Wickstrom, Olsson: Advanced Packaging, September 2001)

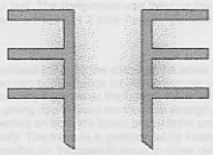

Figure 1. E-pad shaped signal layers used as contact points for ICA joints.

- **E-pads change adhesive failure to cohesive**
- **C-fibers improve impact resistance**

Click here to enlarge image

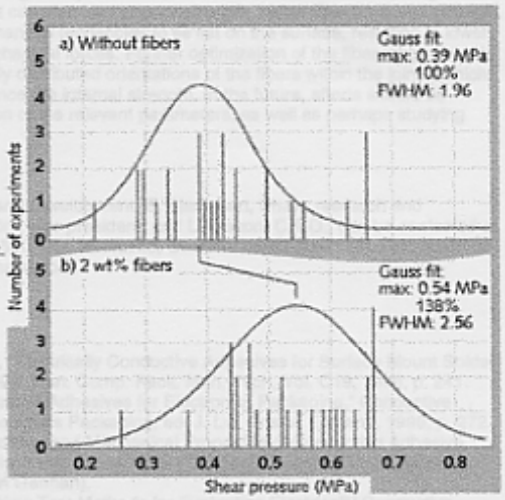

Figure 5. Shear test results of component 1206 dispensed onto E-pads of a test board with pure ICA Y (a) and ICA Y plus 2 weight percent carbon fibers (b). The blue curves represent Gaussian fits onto the raw data (curves are multiplied by a factor of 4).

5.3 Impact Strength/Drop Test

(Tong)

- **Adhesion tests passed**
- **Devices fall off PWB if dropped**
  - **Large devices fail; small OK**
- **No correlation between drop test results and adhesion strength testing**
- **Complex shear modulus**
  - **Storage and loss moduli**

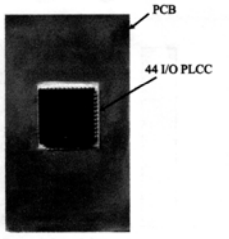

Figure 2. A Photograph of a Drop Test Sample

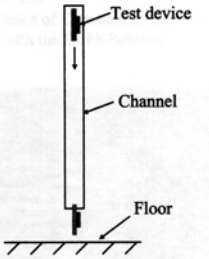

Figure 3. A Schematic of Drop Test Set-up

Variation with inertial mass

Blocks	Drops till failure
1	More than 120 (no failure)
2	30, 43
3	17, 21
4	7, 4,11
5	4, 4
6	3

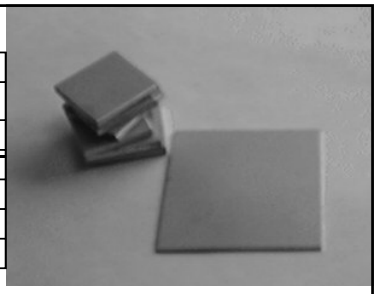

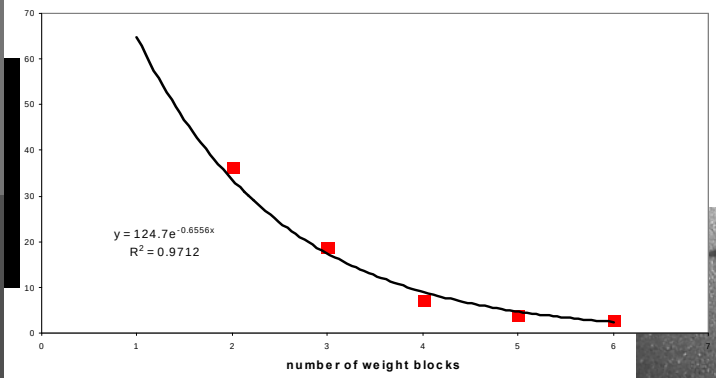

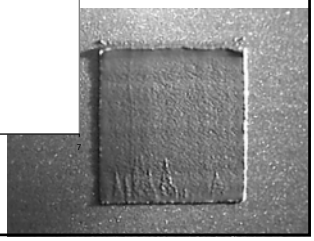

4/27/2009

Shear Stress σ & Strain ε
Complex Shear Modulus

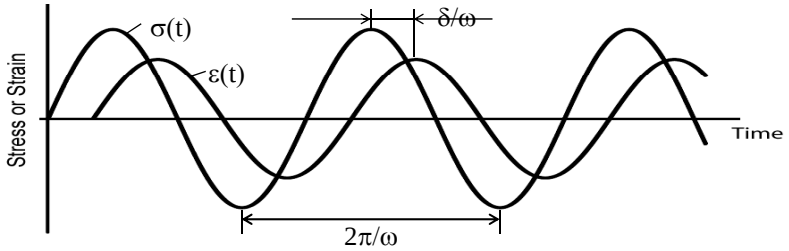

Shear stress $\sigma = S/A$
Shear strain $\varepsilon = a/h$
$\sigma = G\varepsilon$
Elastic shear modulus
$G = G' + iG''$
Loss tangents:
$\tan\delta = G''/G'$

Charge density $\sigma = Q/A$
Electric field $E = V/d$
$\sigma = \varepsilon E \quad [Q = (\varepsilon A/d)V]$
Dielectric constant
$\varepsilon = \varepsilon' + i\varepsilon''$
$\tan\delta = \varepsilon''/\varepsilon'$

Impact Test Data

Table 1. Performance Results

Material	Drop Test Performance	Loss Factor	Tg (°C)
SMCA 1	Fail 36", Fail 60"	0.016	90
SMCA 2	Fail 36", Fail 60"	0.018	80
F - 1	Fail 36", Fail 60"	0.058	40
F - 2	Pass 36", Fail 60"	0.34	20
F - 3	Pass 36", Fail 60"	0.22	-10
F - 4	Pass 36", Pass 60"	0.43	0
F - 5	Pass 36", Pass 60"	0.47	0
S - 1	Pass 36", Pass 60"	0.5	-20
S - 2	Pass 36", Pass 60"	0.32	-15
S - 3	Pass 36", Pass 60"	0.33	-20

- High tanδ by $T_{amb} > T_g \rightarrow$ high CTE

Multiple Drop Testing:

1. Cumulative damage
2. Pre-heat effects

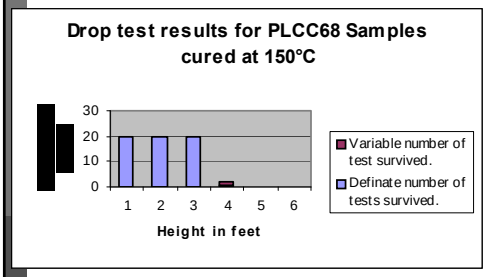

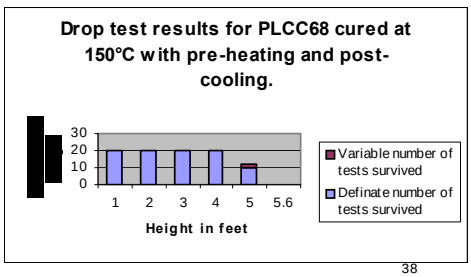

6. Reliability

- 6.1 Testing schedules
- 6.2 Electromigration
- 6.3 Environmental testing: Electrical
  - 6.3.1 Bulk resistance
  - 6.3.2 Contact resistance
  - 6.3.3 Humidity & corrosion
  - 6.3.4 Diffusion
- 6.4 Environmental testing: Mechanical
- 6.5 Thermo-mechanical cycling
- 6.6 Noise
- 6.7 Rapid reliability testing

6.1 Reliability Testing:

Sample test schedule (Danfoss)

- Initial resistance measurement
- Dry heat: 150°C for 1000hours
- Resistance measurement
- Cold storage: +35°C for 1000 hours
- Resistance measurement
- Temperature cycling: 25°C to 90°C 10min/ 10min, 200 cycles
- Resistance measurement
- Humidity cycling, 21 days IEC 68-2-30
- Resistance measurement Adhesion measurement

6.2 Electromigration

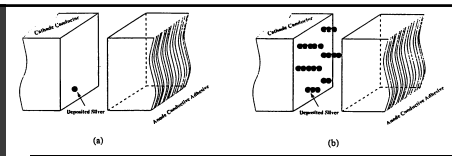

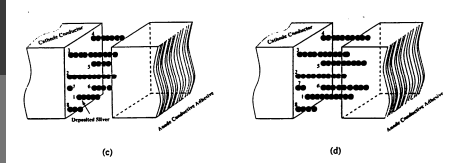

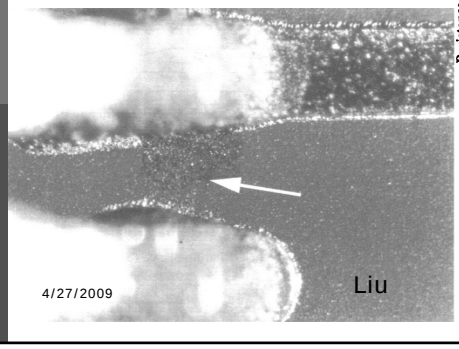

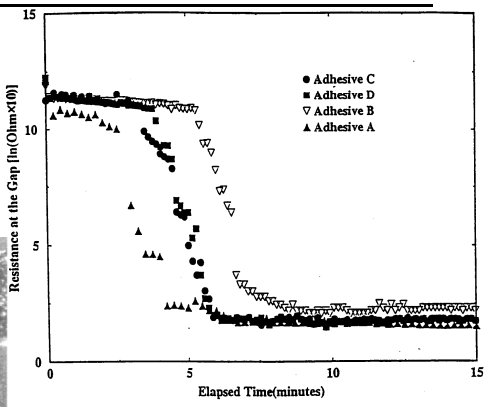

Liu

Sn/Ag alloys ~~inhibit Ag~~ migration

(Suzuki, Polytronic 2004)

(Leakage current (A) for 50V/1.5mm)

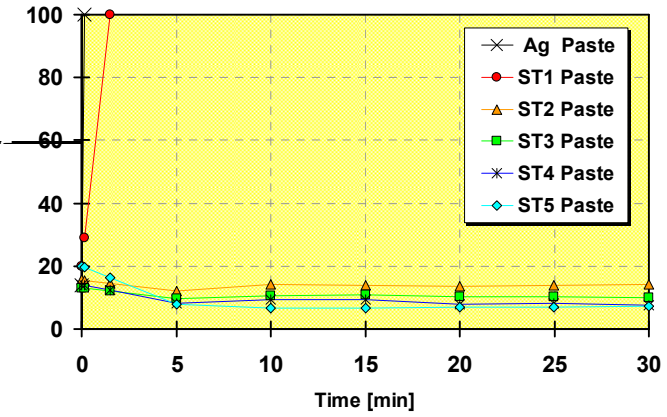

Ag-Sn Powder	Sn Mol %	Mol Ratio Ag	Mol Ratio Sn	Average Particle Diameter
ST1	17.5	3.3	0.7	25 μ m
ST2	25.0	3.0	1.0	25 μ m
ST3	32.5	2.7	1.3	25 μ m
ST4	50.0	2.0	2.0	25 μ m
ST5	75.0	1.0	3.0	25 μ m

Table 1: Ag-Sn Alloy Powders.

Electromigration Reduction with SAMs

[Wong et al, ECTC'06]

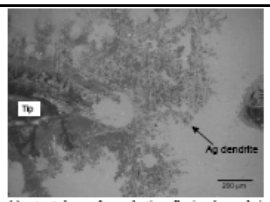

(a) untreated nano-Ag conductive adhesive shows obvious dendrite formation

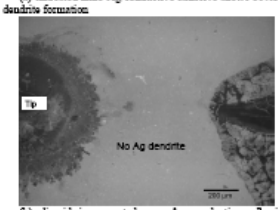

(b) di-acid incorporated nano-Ag conductive adhesive shows no obvious dendrite formation

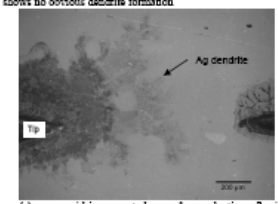

(c) mono-acid incorporated nano-Ag conductive adhesive shows moderate dendrite formation

Fig. 7 Morphology of Ag dendrites after high voltage migration tests. (a) untreated nano-Ag conductive adhesives (b) di-acid incorporated nano-Ag conductive adhesives and (c) mono-acid incorporated nano-Ag conductive adhesives.

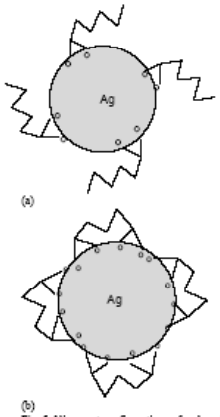

Fig. 5 Alignment configurations of carboxylic acids on Ag particles. (a) mono- acid on Ag particle and (b) di-acid on Ag particle.

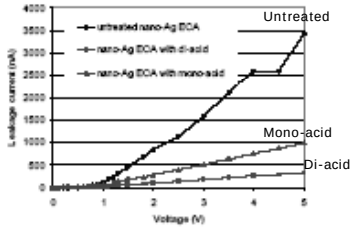

Fig. 3 Leakage current-voltage relationship of nano-Ag conductive adhesives at 0-5 V

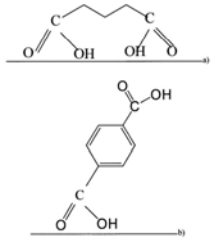

Possible alignment configurations of dicarboxylic acids on silver surfaces

6.3.1 Bulk Resistance 85/85

(Li & Morris)

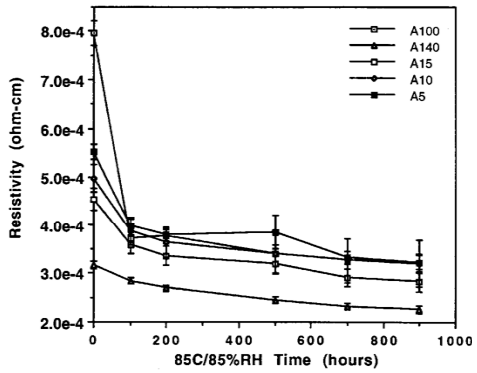

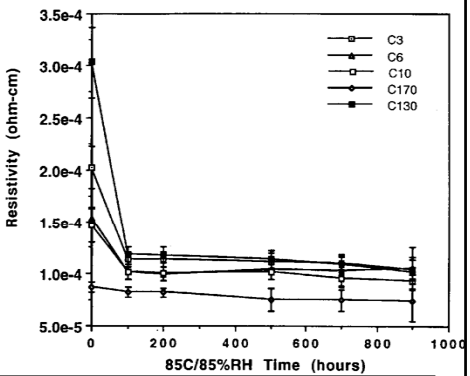

6.3.2 Contact R 85/85: Au & Cu contacts

A on Au

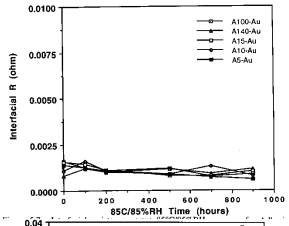

C on Au

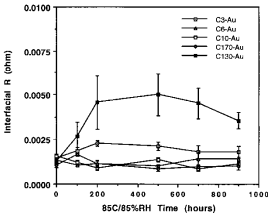

A on Cu

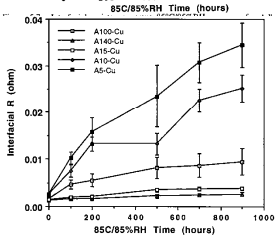

C on Cu

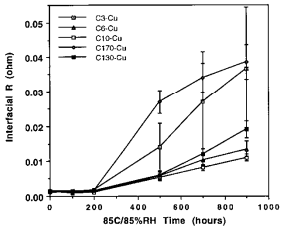

(Li & Morris)

6.3.3. Humidity/Moisture Properties Hygroscopic Swelling

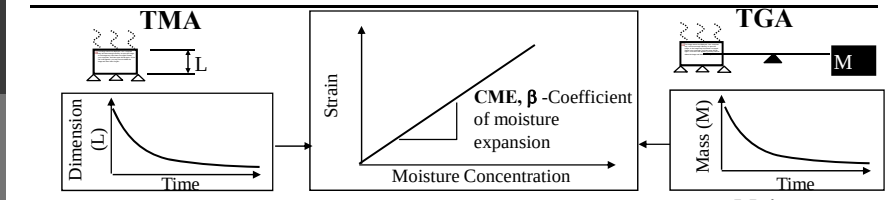

Dimensional reduction | **Combines both measurements** | **Moisture desorption**

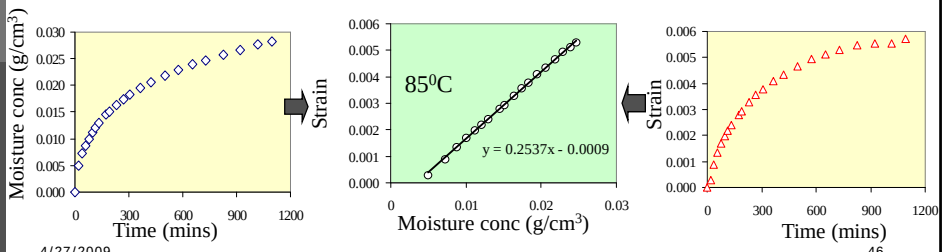

6.3.4 Galvanic Corrosion (Wong/Lu)

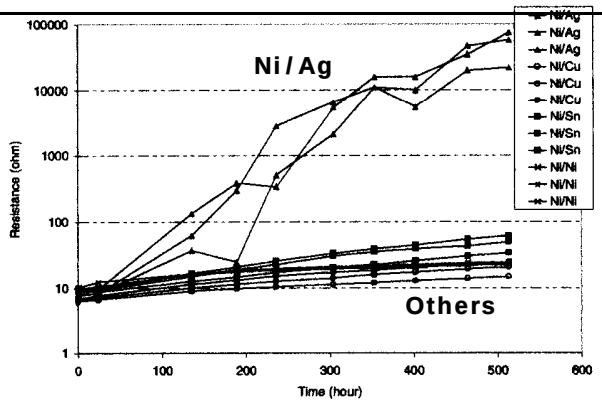

Figure 2. Contact Resistance Shifts of a Ni Flake-filled ECA with Different Metal Wires (Ni, Sn, Cu, and Ag)

Galvanic Corrosion

Electrode Reaction	Normal Potential
$Au - 3e^- = Au^{3+}$	1.50 v
$Pt - 2e^- = Pt^{2+}$	1.20 v
$Ag - e^- = Ag^+$	0.80 v
$Cu - e^- = Cu^+$	0.52 v
$H_2O + O_2 + 4e^- = 4OH^-$	0.40 v
$Cu - 2e^- = Cu^{2+}$	0.34 v
$Pb - 2e^- = Pb^{2+}$	- 0.13 v
$Sn - 2e^- = Sn^{2+}$	- 0.14 v
$Ni - 2e^- = Ni^{2+}$	- 0.25 v

Galvanic Corrosion: Wet/Dry

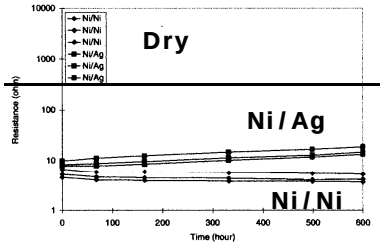

Figure 3. Contact Resistance Shifts of a Ni Flake-filled ICA with Ni and Ag Wires under 85°C/dry Aging Condition.

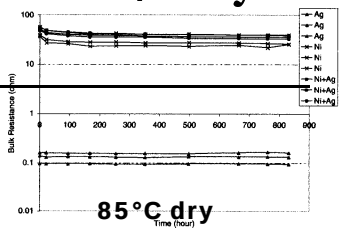

Figure 5. Bulk Resistance Shifts of Three ICAs with Different Fillers under 85°C/dry Aging Condition.

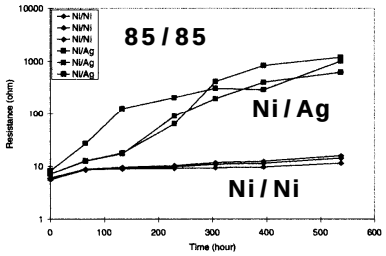

Figure 4. Contact Resistance Shifts of a Ni Flake-filled ICA with Ni and Ag Wires under 85°C/85%RH Aging Condition.

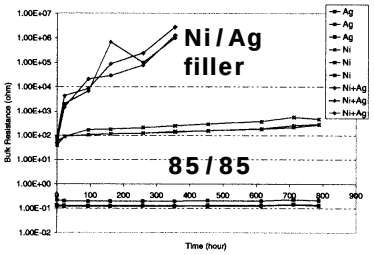

Figure 6. Bulk Resistance Shifts of Three ICAs with Different Fillers under 85°C/85%RH Aging Condition.

Addition of Zn (Takezawa et al: 2002 APM)

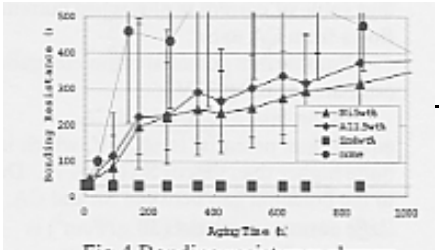

Fig.4 Bonding resistance change (effects of non-noble metals)

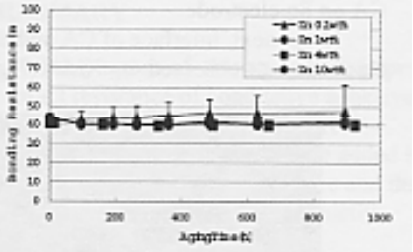

Fig.5 Bonding resistance change (effects of Zn volume)

Table 1 Non-noble metals studied

Non-noble Metals	Normal Potential (V vs NHE)	Shape/Size
Al/Al^{3+}	-1.66	Sphere/7•m
Ni/Ni^{2+}	-0.23	Sphere/5•m
Zn/Zn^{2+}	-0.76	Sphere/7•m
Sn/Sn^{2+}	*-0.14*	•
Ag/Ag^{+}	*+0.80*	•

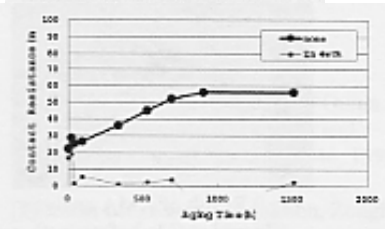

Fig.6 Contact resistance change

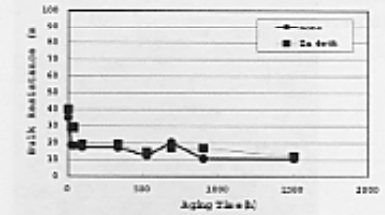

Fig.7 Bulk resistance change

ICA: Lee, Cho, & Morris, Proc. EMAP 2007
Ag-ICA performance comparison on Cu and immersion-Ag PWB contacts